LHCb status and physics goals

Olivier Leroy
Centre de Physique des Particules de Marseille
163 avenue de Luminy Case 907
13288 Marseille cedex 9 France
Email: Olivier.Leroy@in2p3.fr

Abstract

LHCb is a dedicated b-physics experiment which will start to take data on the LHC collider at CERN, in 2007. We present the status of the experiment and some expected physics performance.

1 Physics motivations

LHCb is a dedicated experiment at LHC to study CP violation and other rare phenomena in b-hadrons decays. The b meson sector is a place where theoretical predictions can be precisely compared with experimental results. CP violation is described in the Standard Model by a single complex phase in the CKM matrix [1, 2], which relates the mass-eigenstates to the electroweak eigenstates in the quark sector:

$$V = \begin{pmatrix} V_{\rm ud} & V_{\rm us} & V_{\rm ub} \\ V_{\rm cd} & V_{\rm cs} & V_{\rm cb} \\ V_{\rm td} & V_{\rm ts} & V_{\rm tb} \end{pmatrix} .$$

The matrix can be parametrized with four independent parameters [3]:

$$V \approx \begin{pmatrix} 1-\lambda^2/2 & \lambda & A\lambda^3\,(\rho - i\,\eta) \\ -\lambda & 1-\lambda^2/2 & A\lambda^2 \\ A\lambda^3\,(1-\rho-i\,\eta) & -A\lambda^2 & 1 \end{pmatrix} + \delta V ,$$

where

$$\delta V = \begin{pmatrix} 0 & 0 & 0 \\ -i\,A^2\lambda^5\eta & 0 & 0 \\ A\lambda^5(\rho + i\,\eta)/2 & A\lambda^4(1/2 - \rho - i\,\eta) & 0 \end{pmatrix} .$$

Among the nine unitarity relations of the CKM matrix, the following two are the most relevant for B physics:

$$\begin{aligned} V_{\rm ud}V_{\rm ub}^* + V_{\rm cd}V_{\rm cb}^* + V_{\rm td}V_{\rm tb}^* &= 0\,, \\ V_{\rm tb}V_{\rm ub}^* + V_{\rm ts}V_{\rm us}^* + V_{\rm td}V_{\rm ud}^* &= 0\,. \end{aligned}$$

Using the approximation introduced above, the two relations can be drawn as triangles (see Fig. 1). The parametrization used above implies

$$\arg V_{\rm td} = -\beta, \;\; \arg V_{\rm ub} = -\gamma, \;\; \arg V_{\rm ts} = \chi + \pi\,,$$

In LHCb, we will measure precisely these fundamental parameters of the Model Standard. In addition, we will over constrain the unitarity triangles in order to search for inconsistencies and to exhibit new physics. Indeed new physics scenarii propose new particles and new couplings which can modify the amplitudes of penguin and box diagrams.

To over constrain the unitarity triangles LHCb will have to reconstruct many final states with different topologies: $\mathrm{B}^0 \to \pi^+\pi^-$, $\mathrm{B}^0 \to \mathrm{K}^+\pi^-$, $\mathrm{B_s^0} \to \pi^+\mathrm{K}^-$, $\mathrm{B_s^0} \to \mathrm{K}^+\mathrm{K}^-$, $\mathrm{B_s^0} \to \mathrm{D_s^-}\pi^+$, $\mathrm{B_s^0} \to \mathrm{D_s^\mp K^\pm}$, $\mathrm{B_s^0} \to \mathrm{J}/\psi\phi$, $\mathrm{B_s^0} \to \phi\phi$, $\mathrm{B}^0 \to \mathrm{K}^{*0}\gamma$, ...etc. Final states with hadrons require an efficient and robust trigger for non-leptonic decays. We often need to reconstruct decays with 3 or 4 charged tracks and therefore a high track reconstruction efficiency is mandatory. Channels with $\mathrm{B_s^0}$ need an excellent proper time resolution to resolve the high frequency $\mathrm{B_s^0}$-$\overline{\mathrm{B}}{}_{\mathrm{s}}^0$ oscillation. A very good pion/kaon separation is necessary. These last four points constitute real detector challenges, as it will be shown in the following.

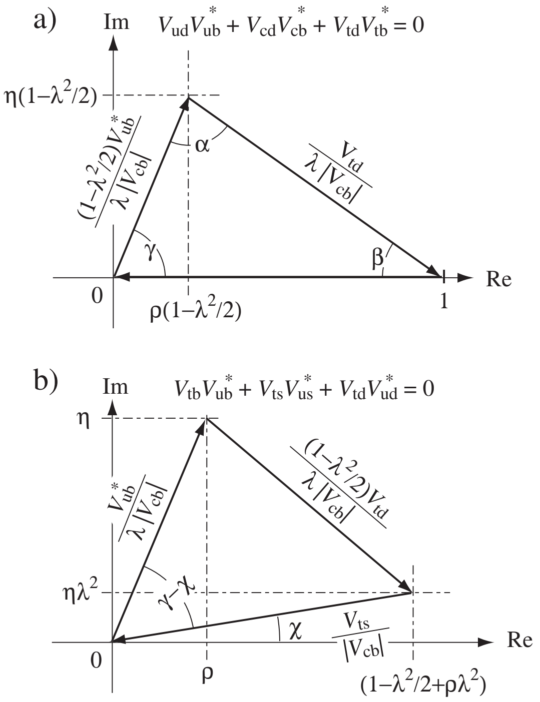

Figure 1: Two unitarity relations drawn in the complex plane: (a) for $V_{\rm ud}V_{\rm ub}^* + V_{\rm cd}V_{\rm cb}^* + V_{\rm td}V_{\rm tb}^* = 0$, and (b) for $V_{\rm tb}V_{\rm ub}^* + V_{\rm ts}V_{\rm us}^* + V_{\rm td}V_{\rm ud}^* = 0$.

The LHC will collide proton-proton with a center-of-mass energy of 14 TeV. Bunches cross at 40MHz. The design LHC luminosity is 10^{34} cm^{-2}s^{-1}, which means more than 20 pp interactions per crossing, since the inelastic pp cross-section is 80mb. This is very difficult to analyse, for example in the case one tries to tag the initial flavour of a b-meson. Therefore, the beams will be defocused[1] at LHCb interaction point to get a luminosity of 2×10^{32} cm^{-2}s^{-1}. Doing this, we will be dominated by single interations and we will also reduce the radiation dose received by the subdetectors. The $b\bar{b}$ cross-section at 14 TeV is 500 μb. In 2007, LHC will be the most copious source of b-hadrons production in the world, with 10^{12} $b\bar{b}$ pairs produced each year. This includes all species of b-hadrons: B^+, B^0, B_s^0, B_c^+, Λ_b, Ξ_b, ...etc.

Figures 2 shows the angular correlation of the b-hadrons produced at LHC, simulated with the PYHTIA program. They indicate that the two b-hadrons are likely to be produced forward. With a very cost-effective solution like a single arm spectrometer LHCb, about 15% of the $b\bar{b}$ events have both b-hadrons in the acceptance. This is essential for b-flavour tagging. Indeed, we can select one B decay of interest and use the other b-hadron to tag the initial flavour. The reduced acceptance compared to the 4-pi detectors like ATLAS or CMS is largely compensated by the detector specifications, as we will see later. In addition, the large boost of the b-hadron in the forward direction will facilitate the detection of detached vertices.

2 The Detector: status of the subsystems

Figure 3 shows the layout of the LHCb detector [4]. The basic layout of the spectrometer consists of a Vertex Locator, dipole magnet, tracking system, two Ring Imaging Cherenkov detectors (RICH 1 and RICH 2) with three radiators, calorimeter system and muon system [5, 6, 7, 8, 9, 10, 11]. The inner acceptance (10mrad) is given by the beam pipe while the outer acceptance is limited by the available room in the DELPHI cavern: 300 (250) mrad in the bending (non-bending) plane.

[1] More precisely, the beams will not be as focused as they are for ALTAS and CMS

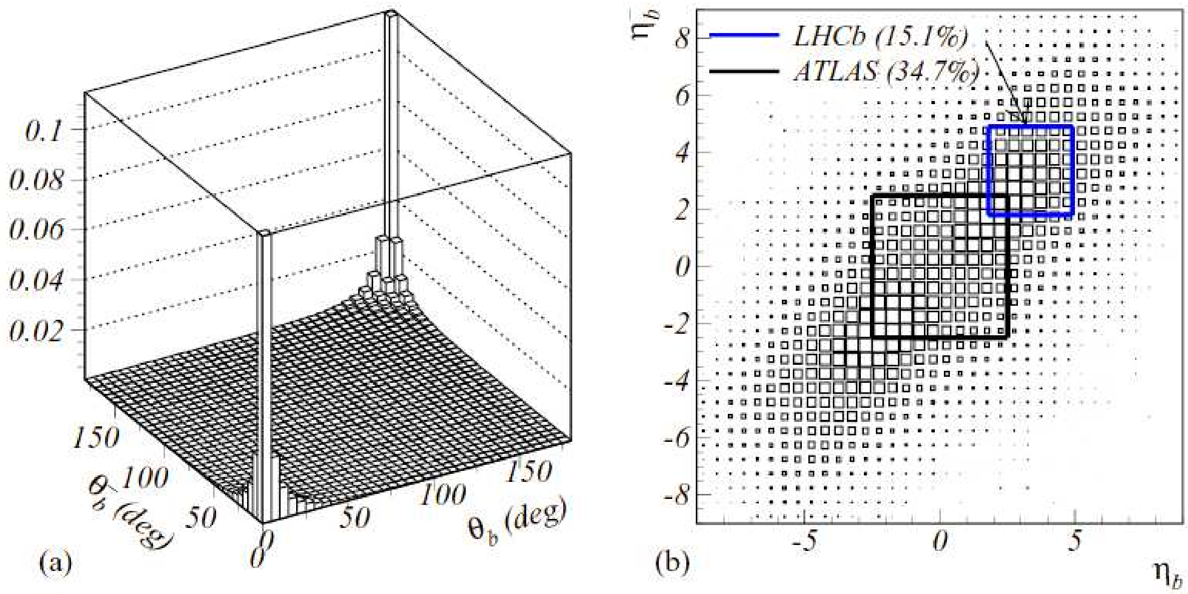

Figure 2: The angular correlation of the two b-hadrons is shown, in terms of (a) the polar angle and (b) the pseudo-rapidity.

2.1 Beam pipe

The beam pipe design is particularly delicate since the vacuum chamber is located in the high rapidity region of the LHCb detector where the particle density is high. The number of secondary particles in an event depends on the amount of material seen by incident primary particles. The mass ot the beam pipe and the presence of flanges or bellows has direct influence on the occupancy, in particular for tracking chambers and the RICH. On June 2004, the first 25mrad Beryllium cone of the beam pipe has been qualified as the final product, while the 2 other sections are ordered.

2.2 Magnet

The assembly of the magnet yoke is completed and the magnet will be moved in its final position during July 2004. We will then perform precise field map measurements, inside the magnet, but also in RICH1, VELO and tracking stations region. The magnet provides a field of 4 T m and is warm to allow regular reversion of the field, in order to reduce experimental systematics on the CP measurements.

2.3 Vertex Locator

The vertex locator has to provide precise measurements of track coordinates close to the interaction region. It is optimised to give the best impact parameter resolution with the smallest amount of material. The VELO consists of 21 silicon stations placed along the beam direction. This device contains 3 additional silicon disks used in the level-0 trigger to reject multiple proton-proton interactions. The sensors arrangements is shown on Fig. 4. The sensors are placed at a radial distance of 8 mm from the beam and can be retracted during injection. For minimizing the material between the interaction region and the detectors, the silicon sensors are inside a thin aluminium box with a pressure of less than 10^{-4}mbar. The side of the box facing the beam also shields the sensors against RF pickup. Each of the 21 VELO station consists of 2 sensors, 220 μm thin, one with R strips, the other with ϕ strips. The strip piches goes from 35 to 102 μm. The expeced impact parameter resolution is 30 μm. The VELO data represent 180,000 readout channels. The sensors are equipped with 12 frond-end chips. The final chips production

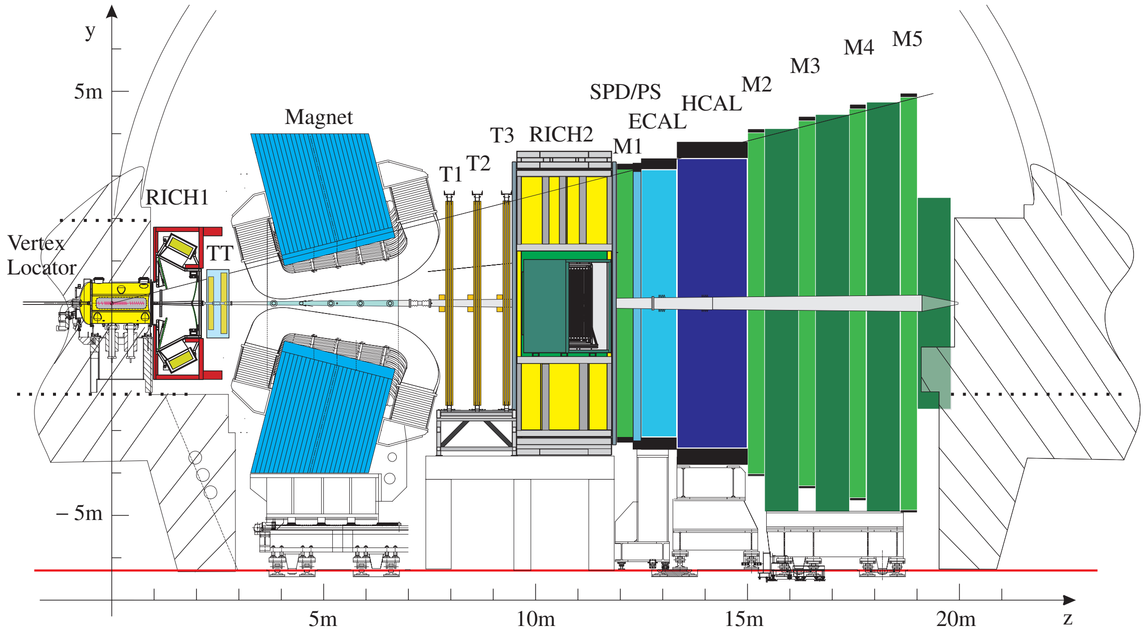

Figure 3: LHCb detector layout in the $y-z$ plane, showing the Vertex Locator (VELO), the dipole magnet, the two RICH detectors, the four tracking stations TT and T1–T3, the Scintillating Pad Detector (SPD), Preshower (PS), Electromagnetic (ECAL) and Hadronic (HCAL) calorimeters, and the five muon stations M1–M5.

will start in October 2004. The sensors are already in production. The mechanics of the VELO is also well advanced.

2.4 Other tracking stations (TT, T1, T2, T3)

The tracking system has to provide a momentum resolution below half a percent to give a B mass resolution below 15 MeV. In addition to the VELO, the trigger tracker "TT" is placed before the magnet and 3 other trackers called T1, T2 and T3, downstream of the magnet.

TT is used in level-1 trigger to assign transverse-momentum information to large-impact parameter tracks. It is also used in offline analysis to reconstruct the trajectories of long-lived neutral particles that decay ouside the VELO and of low-momentum particles that are bent out of the acceptance before reaching T1. TT is made of 2+2 layers separated by 30 cm. Each layer is made of silicon strips 500 μm thin with a pitch of 193 μm. This represents 144k channels to read.

The stations T1 to T3 are splitted into 2 main components. The inner part is equipped with silicon strip to face high occupancy and radition dose. There are 4 layers per station, each with 320 μm thin silicon and 198 μm readout pitch. The outer part is equipped with 5 mm straw tubes, arranged in 4 double layers. This represents 50k readout channels.

The sensors of the inner tracker have been ordered. The TT ladder prototype is being finalized and TT sensors order is being prepared. The straw tube production for the Outer Tracker has started.

The performance of the tracking system is the following: 27 tracks which traverse the full spectrometer are reconstructed per event. The efficiency is 94% for tracks above 10 GeV and the momentum resolution is 0.4%. The resolution on the impact parameter of the tracks with respect to the primary vertex peaks at 20 μm, and its average is 40 μm.

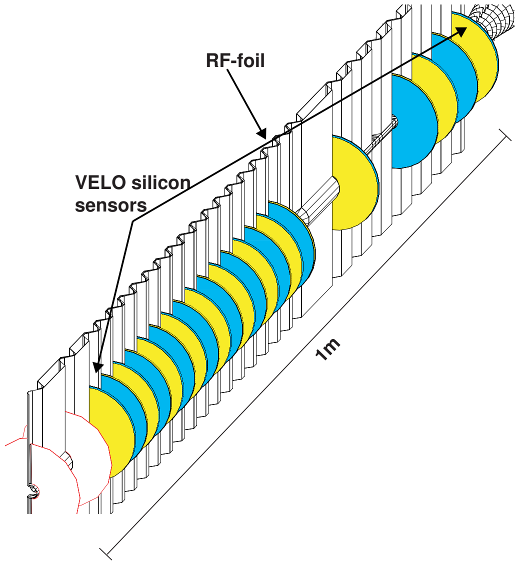

Figure 4: Arrangements of detectors along the beam axis. Only the silicon sensors on one side of the RF-foil, which separates the LHC vacuum from the detector vacuum, can be seen. The first two detectors (unshaded) belong to the Pile-Up system [12].

2.5 Ring Imaging Cerenkov detectors

In LHCb charged hadrons over a large momentum range up to 150 GeV must be identified as well as low momemta particles such as the kaons used in tagging. There is a strong correlation between the polar angle and momentum of the tracks. At wide angle, the momentum spectrum is softer. The Ring Imaging Cerenkov detector (RICH) is therefore divided into two detectors.

Low momentum particles between 1 and 60 GeV are identified by RICH1. It combines silica aerogel and fluorocarbon gas radiator with a polar acceptance from 25 to 300mrad. A significant fringe field between the VELO and the trigger tracker station is required to determine the momenta of particles in the level-1 trigger. This imposed strong constraints on the RICH1 design, especially an efficient shielding the photodetectors.

High momentum particles (up to 100 GeV) are identified by RICH2 located downstream of the magnet and tracking stations. The radiator used is CF_4. The RICH2 superstructure is completed as well as the entrance/exit windows and 10% of RICH2 mirrors are produced and tested. The photodectors technology has been chosen on the basis of beam tests results and Hybrid PhotoDiods (HPDs) have been ordered.

A 3σ separation between pions and kaons is expected for a momentum between 3 and 80 GeV.

2.6 Calorimeters

The calorimeter system provides identification of electrons, hadrons, and neutral particles. It is also used in the level-0 trigger. It consists of a Scintillating Pad Detector, a PreShower (PS), a shashlik electromagnetic calorimeter and a hadron calorimeter made of steel and scintillating tiles. The PreShower is made of lead converter, sandwiched between two scintillator planes with 16,000 scintillating pads. The electromagnetic calorimeter is made of layers of lead and scintillator. The readout is done via Wave Length Shifter fibres and the energy resolution is about $10\%/\sqrt{E}$. All the ECAL modules have been delivered. The HCAL is a sandwich of iron and scintillator. The energy resolution is $\sim 75\%/\sqrt{E}$. 60% of modules are completed and the installation of both ECAL and HCAL is scheduled for november 2004.

2.7 Muon detectors

The muon system provides muon identification and is also crucial for the level-0 trigger. It consists of 5 stations interlaid with iron shield. The stations are multiwire proportional chambers, except in inner region of station 1, where GEM are used because of the high rate. The efficiency to find a muon from B decays is around 95% for a pion misdentification rate below 1%.

The production of the 1400 multi-wire-proportional chambers for the 5 stations is on the way. The iron muon filter is being mounted on its chariot in the experiment hall.

2.8 Trigger and data acquisistion

The trigger has to reduce a 40MHz input rate to roughly 200 Hz, while keeping as many interesting b-events as possible. This is achieved in 3 steps: the level-0 trigger is a customed hardware processor which uses high p_T electrons, muons and hadrons to reduce the rate to 1 MHz. The following step uses impact parameter and p_T of the tracks to refine the selection of B-candidates. The rate is reduced to 40kHz. The last step performs a full event reconstruction to select b decays of interest. The last 2 steps run on the same CPU farm. The level-0 times level-1 efficiency varies between 40 to 90%, depending on the physics channel of interest. Prototype of trigger hardware is ready and the construction phase will start in 2005.

3 Physics potential

3.1 Framework and annual event yield and tagging performance

Physics potential of LHCb is estimated using Monte Carlo simulation. Proton-proton collisions are generated using PYTHIA 6.2. Hard QCD processes, single and double diffraction are included. Multiple parton interactions are tuned to reproduce the track multiplicities observed at SPS and Tevatron energies. The particles are propagated through the detector using Geant3 simulation. Each sub-dector response, resolution, efficiency, noise and cross-talk is taken into account using test beam data. Then the offline reconstruction is done using a full pattern recognition program, including track finding and RICH reconstruction.

The physics performance mentionned in this paper have been obtained with 67M events simulated in 2003, among which 10M $\mathrm{b\bar{b}}$ events have been generated to study what is considered as the most dangerous background. Note that this corresponds only to 4 minutes of real data taking. This year, an improved simulation has been developed and a new massive events production is on the way with 5 times more $\mathrm{b\bar{b}}$ events.

Table 1 summarizes the untagged signal yield and background-over-signal estimates for various B-decays, in 1 year of LHCb data taking (2fb^{-1}) [4].

Various information is used to tag the inital b-flavour of the selected hadron: muon, electron or kaon from the other b-hadron, vertex charge of the other b-hadron, fragmentation kaon from the same side of the reconstructed $\mathrm{B_s^0}$. Performance of the b-flavour tagging is illustrated in Table 2. This table gives the tagging efficiency (ϵ_{tag}) and the mistag probability (ω)for various categories, together with the effective efficiency defined as $\epsilon_{\mathrm{tag}}(1-2\omega)^2$. The combined effective efficiency is roughly 4% for fully reconstructed $\mathrm{B^0}$ and 6% for $\mathrm{B_s^0}$. Work is on-going to improve these results.

3.2 Δm_{s}

To measure time-dependent CP asymmetries with $\mathrm{B_s^0}$ mesons, one first needs to measure Δm_{s}, the oscillation frequency. This will be done using $\mathrm{B_s^0} \to \mathrm{D_s^-}\pi^+$ decays. If Δm_{s} is equal to 20 ps^{-1}, the statistical uncertainty will be 0.01ps^{-1}. We can observed Δm_{s} at 5σ up to 68ps^{-1} thanks to the excellent proper time resolution, typically below 40fs. LHCb will therefore explore Δm_{s}values well above the range predicted by the Standard Model (15-25 ps^{-1}) and well above the present experimental limit (Δm_{s}>14.4 ps^{-1}).

Table 1: Summary of the untagged annual signal yields and background-over-signal (B/S) ratios from inclusive $b\overline{b}$ events. The annual signal yields include both the indicated decays and their charge conjugates. Quoted errors on B/S are from the Monte Carlo statistics; estimates based on less than 10 Monte Carlo background events are quoted as 90% CL upper limits.

Decay channel	Annual signal yield (k)	B/S
$B^0 \to \pi^+\pi^-$	26.	< 0.7
$B^0 \to K^+\pi^-$	135.	0.16 ± 0.04
$B_s^0 \to \pi^+K^-$	5.3	< 1.3
$B_s^0 \to K^+K^-$	37.	0.31 ± 0.10
$B^0 \to \rho\pi$	4.4	< 7.1
$B^0 \to D^{*-}\pi^+$	206.	< 0.3
$B^0 \to \overline{D}^0(K\pi)K^{*0}$	3.4	< 0.5
$B^0 \to D^0_{CP}(KK)K^{*0}$	0.59	< 2.9
$B_s^0 \to D_s^-\pi^+$	80.	0.32 ± 0.10
$B_s^0 \to D_s^\mp K^\pm$	5.4	< 1.0
$B^0 \to J/\psi(\mu\mu)K_S^0$	216.	0.80 ± 0.10
$B^0 \to J/\psi(ee)K_S^0$	25.6	0.98 ± 0.21
$B^0 \to J/\psi(\mu\mu)K^{*0}$	670.	0.17 ± 0.03
$B^+ \to J/\psi(\mu\mu)K^+$	1740.	0.37 ± 0.02
$B_s^0 \to J/\psi(\mu\mu)\phi$	100.	< 0.3
$B_s^0 \to J/\psi(ee)\phi$	20.	0.7 ± 0.2
$B_s^0 \to J/\psi(\mu\mu)\eta$	7.0	< 5.1
$B_s^0 \to \eta_c\phi$	3.2	< 1.4
$B_s^0 \to \phi\phi$	1.2	< 0.4
$B^0 \to \mu^+\mu^-K^{*0}$	4.4	< 2.0
$B^0 \to K^{*0}\gamma$	35.	< 0.7
$B_s^0 \to \phi\gamma$	9.3	< 2.4
$B_c^+ \to J/\psi(\mu\mu)\pi^+$	14.0	< 0.8

Table 2: Tagging performance for $B^0_{(s)} \to h^+h^-$ signal events passing trigger and offline cuts. Uncertainties are statistical only.

Tag	ε_{tag} (%)	w (%)	ε_{eff} (%)
μ	11.1±0.3	35.3±1.1	1.0±0.2
e	5.2±0.2	35.6±1.7	0.4±0.1
K_{opp}	16.6±0.3	31.2±0.9	2.4±0.2
Q_{vtx}	24.3±0.6	39.9±0.8	1.0±0.2
Combined (B^0)	40.9±0.4	34.6±0.7	3.9±0.3
K_{same}	17.5±0.4	32.8±1.2	2.1±0.3
Combined (B^0_s)	49.8±0.5	32.8±0.8	5.9±0.5

3.3 ϕ_s=2χ

The B^0_s mixing phase, ϕ_s, will be measured using the CP asymmetry in $B^0_s \to J/\psi\phi$ events. This channel is the B^0_s counterpart of the golden mode $B^0 \to J/\psi K^0_S$. The J/ψ is reconstructed in $\mu^+\mu^-$ or e^+e^- and the ϕ in K^+K^- Here an angular analysis of the decays products is necessary to separate the CP-even from the CP-odd contributions. The standard model predicts ϕ_s around 0.04 rad. If Δm_s is for example equal to 20 ps^{-1}, the statistical uncertainty on sinϕ_s after 1 LHCb year will be 0.06 rad.

3.4 Three methods to measure γ

The γ angle can be measured with at least 3 methods, each having different sensitivity to new physics.

- Method I. $\gamma + \phi_s$ from $B^0_s \to D^\mp_s K^\pm$

In the first one, inteference between the 2 tree diagrams and $B^0_s\overline{B}^0_s$-mixing in $B^0_s \to D^\mp_s K^\pm$ allows the extraction of $\gamma + \phi_s$, from the 2 time-dependent decays rates (Fig. 5). The mistag fraction can be extracted from $B^0_s \to D^-_s\pi^+$ sample and ϕ_s is measured with $B^0_s \to J/\psi\phi$. Uncertainty on γ is estimated to be 14-15 degrees after one year of data taking. This assumes Δm_s=20 ps^{-1}, $\Delta\Gamma_s = 0.1$, γ between 55 and 105 degrees and the strong phases difference between the 2 tree diagrams below 20 degrees. This channel has no theoretical uncertainties and is insensitive to new physics in B^0_s mixing.

- Method II. γ from $B^0 \to \pi^+\pi^-$ and $B^0_s \to K^+K^-$

γ can also be measured using $B^0 \to \pi^+\pi^-$ and $B^0_s \to K^+K^-$ decays which are governed by b→u processes with large b→d(s) penguin contributions [14]. One needs to measure the time-dependent CP asymmetries in these 2 channels, given by the relation:

$$\mathcal{A}_{CP} = \mathcal{A}^{dir}\cos(\Delta m t) + \mathcal{A}^{mix}\sin(\Delta m t)$$

In the Standard Model, $\mathcal{A}^{dir}_{\pi\pi}$ and $\mathcal{A}^{mix}_{\pi\pi}$ can be expressed as

$$\begin{aligned} \mathcal{A}^{dir}_{\pi\pi} &= \frac{2d\sin\vartheta\sin\gamma}{\xi}\,, \\ \mathcal{A}^{mix}_{\pi\pi} &= -\frac{1}{\xi}\left[\sin(\phi_d+2\gamma) - 2d\cos\vartheta\sin(\phi_d+\gamma) + d^2\sin\phi_d\right], \end{aligned}$$

with

$$\xi = 1 - 2d\cos\vartheta\cos\gamma + d^2\,,$$

where the hadronic parameters d and ϑ represent the magnitude and phase of the penguin-to-tree amplitude ratio of the decay transition [14]. Analogously, $\mathcal{A}^{dir}_{KK}$ and $\mathcal{A}^{mix}_{KK}$ can be written as:

$$\mathcal{A}^{dir}_{KK} = -\frac{2\widetilde{d'}\sin\vartheta'\sin\gamma}{\xi'}\,,$$

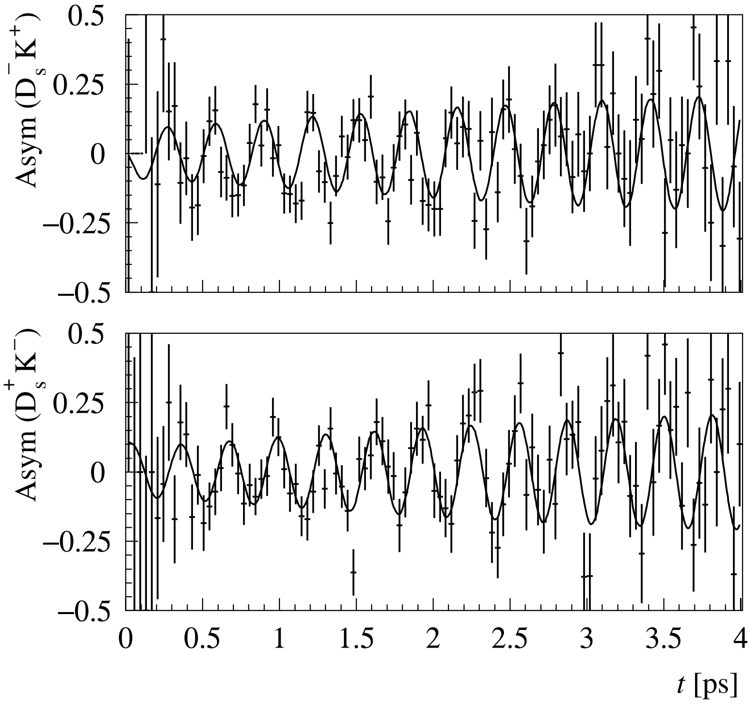

Figure 5: Time-dependent $\overline{B}^0_s$-B^0_s asymmetry of simulated $D_s^- K^+$ (top) and $D_s^+ K^-$ (bottom) candidates for $\Delta m_s = 20$ ps^{-1}. The data points represent five years of data, while the curves correspond to the maximized likelihood.

$$\mathcal{A}_{\rm KK}^{\rm mix} \quad = \quad -\frac{1}{\xi'}\left[\sin(\phi_{\rm s}+2\gamma) + 2\widetilde{d'}\cos\vartheta' \sin(\phi_{\rm s}+\gamma) + \widetilde{d'}^2 \sin\phi_{\rm s}\right],$$

with

$$\xi' = 1 + 2\widetilde{d'}\cos\vartheta'\cos\gamma + \widetilde{d'}^2 ,$$

where $\widetilde{d'} = d'\,(1-|V_{\rm us}|^2)/|V_{\rm us}|^2$, and d' and ϑ' are the analogs of d and ϑ for the $B^0_s \to K^+K^-$ decay. Assuming U-spin flavour symmetry one has 4 measurements and 3 unknowns, which allow to extract γ. The mistag fraction will be extracted from $B^0 \to K^+\pi^-$ and $B^0_s \to \pi^+K^-$ and $\phi_{\rm d}$ and $\phi_{\rm s}$ from the expected LHCb precison measurements. From this study, LHCb expects an uncertainty on γ of 4-6 degrees in one year of data taking. This channel is sensitive to new physics in the penguins.

- Method III. γ from $B^0 \to \overline{D}^0 K^{*0}$, $D^0 K^{*0}$

γ can also be extracted using $B^0 \to \overline{D}^0 K^{*0}$ decays, exploiting the interference between the 2 tree diagrams [15]. The method consists in measuring the six time-integrated rates:

$$\begin{aligned}
\Gamma_+ &= \Gamma(B^0 \to D^0 K^{*0}),\\
\Gamma_- &= \Gamma(B^0 \to \overline{D}^0 K^{*0}),\\
\Gamma_{\rm CP} &= \Gamma(B^0 \to D^0_{\rm CP} K^{*0}),\\
\overline{\Gamma}_+ &= \Gamma(\overline{B}^0 \to D^0 \overline{K}^{*0}),\\
\overline{\Gamma}_- &= \Gamma(\overline{B}^0 \to \overline{D}^0 \overline{K}^{*0}),\\
\overline{\Gamma}_{\rm CP} &= \Gamma(\overline{B}^0 \to D^0_{\rm CP} \overline{K}^{*0}).
\end{aligned}$$

No proper time measurement or tagging is required. With this method, the statistical uncertainty on γ is 7-8 degrees in one year of data. The method has no theoretical uncertainties and is sensitive to new phase in $D^0\overline{D}^0$-mixing.

If there is no new physics affecting the B meson system via loop processes, the three methods presented

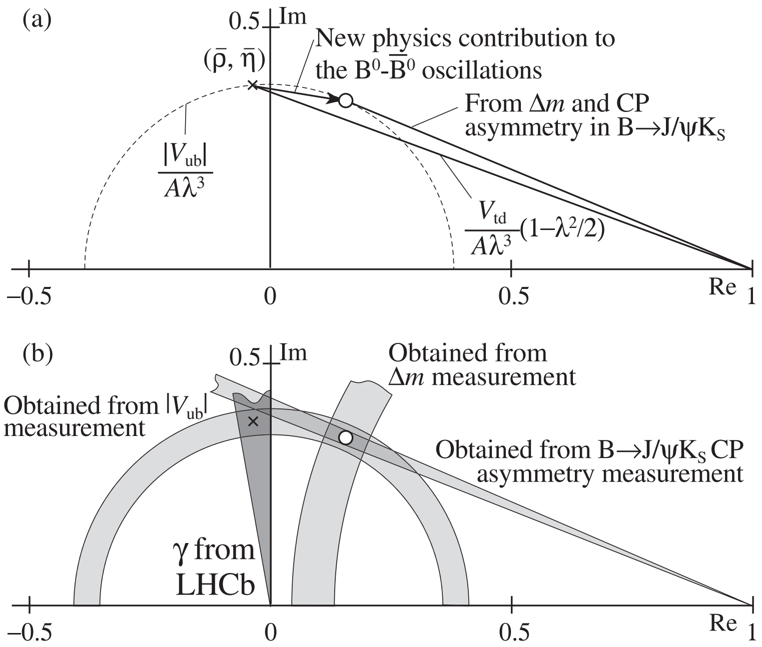

Figure 6: The CKM parameters $\bar{\rho}$ and $\bar{\eta}$ in the complex plane including the effect due to possible new physics: (a) The point marked by $\times$ is the CKM parameter position $(\bar{\rho},\, \bar{\eta})$ and the open circle indicates the currently favoured $(\bar{\rho},\, \bar{\eta})$ from the Standard Model analysis based on $|V_{\rm ub}|$, $\Delta m_{\rm d}$ and CP asymmetry in $B^0 \to J/\psi K^0_S$ decays. The new physics contribution is also indicated. (b) Possible picture with LHCb results for γ from Methods I and II after one year of data taking.

before should measure the same value of γ. The current determination from CKM fit gives $\gamma \approx 65°$. However, if new physics plays a role, the situation might be different. To illustrate a possible scenario, let us assume that the B^0–$\overline{B}^0$ oscillation amplitude is affected by new physics, in such a way that the new physics contribution to $\Delta m_{\rm d}$ is about -30% of the Standard Model contribution, with a phase difference of a few degrees compared to the Standard Model. This could then lead to $\gamma \approx 95°$. In this situation, illustrated in Fig. 6 (a), the constraints from the current measurements of $\Delta m_{\rm d}$ and the CP asymmetry between B^0 and $\overline{B}^0$ decaying to $J/\psi K^0_S$ would still give, together with the $|V_{\rm ub}|$ measurement, the solution shown as a open circle.

For this scenario, Method I will measure $\gamma = 95°$ since it gives the phase of $V_{\rm ub}$ even if new physics contributes to the oscillations. Similarly, Method II will provide $\gamma = 95°$, if the U-spin symmetry is valid. Thus, the LHCb experiment will measure the real value of γ (different from 65°) with an accuracy of better than 5° with the first year of data taking. Figure 6 (b) illustrates the LHCb measurement, which would clearly signal the existence of new physics in the B–$\overline{B}$ oscillations and allow to separate the contributions from the Standard Model and from new physics. It is interesting to note that the value of γ measured by Method III reveals whether new physics also affects the D^0–$\overline{D}^0$ mixing.

If instead new physics appears in the $b \to d$ penguin diagrams, the currently known CKM parameters are the correct values, and the γ measurements from Methods I and III will give $\gamma \approx 65°$. However, the γ measurement from Method II will yield a different value.

Finally new physics may contribute to both the oscillations and penguin diagrams. Method I will still yield the correct value of γ, while Method II will give a value different from the CKM parameters. Again the result of Method III, when compared to that of Method I, will indicate whether new physics appears in the D^0–$\overline{D}^0$ mixing.

This demonstrates how these three different γ measurements in LHCb could isolate new physics.

4 Conclusion

LHCb is a dedicated experiment at LHC to study B physics with a dedicated trigger, an excellent vertex and momentum resolution and particle identification. The construction of the detector is progressing well and it will be ready for the first LHC collision in 2007. LHCb will give unprecedented statistics for B decays, including access to B_s^0 meson, unavailable to the B factories. B_s^0-$\overline{B}_s^0$ oscillation will be measured precisely up to 68 ps^{-1}. Many measurements of rare decays and CP asymmetries will be performed. The expected statistical uncertainty on sin2β after one year of data taking is 0.02; 0.06 for sinϕ_s and below 10 degrees for γ.

CP angles will be determined via channels with different sensitivity to new physics, so that detailed tests of the CKM description of the quark sector will be possible.

As a conclusion, LHCb offers an excellent opportunity to spot new physics signal beyond Standard Model, very soon at LHC

Acknowledgments

I would like to thanks the organizers of QFTHEP'04 for the invitation and many of my LHCb collegues for helping in preparing this talk, in particular Tatsuya Nakada, Olivier Schneider and Roger Forty.

References

[1] T. Maskawa et M. Kobayashi, *"CP-Violation in the Renormalizable Theory of Weak Interaction"*, Prog. Th. Phys. **49** (1973) 652.

[2] N. Cabibbo, *"Unitarity Symmetry and Leptonic Decays"*, Phys. Rev. Lett. **10** (1963) 531

[3] L. Wolfenstein, Phys. Rev. Lett. **51** (1983) 1945

[4] LHCb Collaboration, "LHCb Reoptimized Detector and Performance TDR" , CERN/LHCC 2003-30, LHCb TDR 9, 9 Sep 2003.

[5] LHCb Collaboration, "LHCb VELO Technical Design Report", CERN/LHCC/2001-011, LHCb TDR 5, 31 May 2001.

[6] LHCb Collaboration, "LHCb magnet Technical Design Report", CERN/LHCC/2000-007, LHCb TDR 1, 17 December 1999.

[7] LHCb Collaboration, "LHCb Inner Tracker Technical Design Report", CERN/LHCC/2002-029, LHCb TDR 8, November 2002.

[8] LHCb Collaboration, "LHCb Outer Tracker Technical Design Report", CERN/LHCC/2001-024, LHCb TDR 6, 14 September 2001.

[9] LHCb Collaboration, "LHCb RICH Technical Design Report", CERN/LHCC/2000-0037, LHCb TDR 3, 7 September 2000.

[10] LHCb Collaboration, "LHCb calorimeters Technical Design Report", CERN/LHCC/2000-0036, LHCb TDR 2, 6 September 2000.

[11] LHCb Collaboration, "LHCb Muon system Technical Design Report", CERN/LHCC/2001-010, LHCb TDR 4, 28 May 2001.

[12] LHCb Collaboration, "LHCb Trigger TDR", CERN/LHCC 2003-31, LHCb TDR 10, 9 Sep 2003.

[13] LHCb Collaboration, "LHCb Online System Technical Design Report: Data Acquisition and Experiment Control System", CERN/LHCC/2001-040, LHCb TDR 7, December 2001.

[14] R. Fleischer, Phys. Lett. B **459** (1999) 306

[15] M. Gronau and D. Wyler, Phys. Lett. B **265** (1991) 172;
I. Dunietz, Phys. Lett. B **270** (1991) 75